# Exchange splitting of image states on Fe/Cu(100) and Co/Cu(100)

W. Wallauer and Th. Fauster*
*Sektion Physik, Universität München, Schellingstrasse 4, D-80799 München, Germany*
(Received 2 February 1996)

The image states on epitaxial films of iron and cobalt on Cu(100) have been investigated. For iron the energies can be related to the variation of the film morphology with coverage due to the extreme surface sensitivity of the image states. With the help of spin-selective excitations of electrons into the image states, the exchange splitting of the first image state on 7 ML of Fe on Cu(100) could be determined to $65\pm15$ meV. The exchange splitting for a 6-ML Co film is $55\pm10$ meV. These results are in agreement with a ferromagnetic order of the surfaces and can be obtained without magnetization of the sample. [S0163-1829(96)07431-0]

## I. INTRODUCTION

The deposition of iron on Cu(100) substrates at room temperature leads to the growth of fcc Fe/Cu(100) films.[1,2] Many investigations concerning this adsorbate system have been performed in the past years, yielding rather contradictory results about the growth mode[3–5] and magnetic behavior[5–8] of these films. Different preparation procedures might have been one reason for these discrepancies.

For an understanding of the complex magnetic behavior of these films[5,8] information about the surface electronic structure is needed. Electronic surface states play an important role in the determination of the magnetic and structural properties and offer a convenient way to study the spin-dependent electronic structure at magnetic surfaces.[9] A particular type of surface state has its origin in the long-range $1/z$ image potential in front of a metallic surface. These unoccupied states form a Rydberg-like series converging towards the vacuum level. They are called image states and have been under investigation on metallic surfaces for over ten years.[10,11]

We chose these states for two reasons: (i) image states constitute a highly sensitive probe of the geometrical arrangement of an adsorbate system due to their localization some tenths of nanometers in front of a metallic surface.[11–14] (ii) The binding energies of image states depend decisively on their energetic position within the band gap of the same symmetry. The exchange splitting of the band-gap edges causes, therefore, an exchange splitting of the image states. From the magnitude of this splitting, one can draw conclusions about the spin-dependent electronic structure and surface potential of the investigated magnetic surfaces. Such splittings have already been observed in earlier investigations by spin-resolved inverse photoemission.[15–17] Due to the rather small overlap of the image states with bulk states, their splitting is much smaller than the splitting of the energy bands of 1.26 eV for bcc Fe(110) (Ref. 18). On this surface the exchange splitting of the first image state was experimentally determined to $57\pm5$ meV (Ref. 17) in perfect agreement with a theoretical calculation.[19] Other theoretical models predict values between 29 meV (Ref. 11) and 100 meV (Ref. 20). Two-photon photoemission[21] offers an energy resolution superior to inverse photoemission. The lack of spin resolution has, however, prevented a determination of the exchange splitting of image states so far. Due to the large intrinsic linewidth of these states at the close-packed magnetic surfaces only an upper limit for the exchange splitting could be given.[22]

Image states on Fe/Cu(100) have already been studied by inverse photoemission.[23] No shifts of the energies of the image states up to a coverage of 21 ML were detected. In our two-photon photoemission study we determine these energetic positions more precisely and correlate the results with the geometrical and morphological arrangement of the surface. Using spin-selective excitations in the two-photon photoemission process we obtain the exchange splitting and the spin-dependent linewidth of the image states for epitaxial fcc Fe and Co films on Cu(100).

## II. EXPERIMENT

The experiments were carried out in an ultrahigh vacuum system described elsewhere[11,24] with a base pressure better than $1\times10^{-8}$ Pa. In our two-photon photoemission setup, pulsed laser light is used to excite electrons from occupied states into unoccupied states below the vacuum level $E_{\mathrm{vac}}$. A second photon lifts these excited electrons above the vacuum level, so they can leave the surface and be detected by an electron spectrometer. A excimer laser delivered pulses of 20-ns duration to a dye laser,[21] which was operated at wavelengths between 535 and 580 nm. The polarization of the photons could be varied by an electro-optical cell without modification of the optical setup and variation of the intensity. The analyzer resolution was set to about 50 meV and only electrons that left the sample normal to the surface were detected. The Cu(100) sample was cleaned by $Ne^+$ sputtering ($1\times10^{-3}$ Pa, 600 eV, 300 K) and subsequent annealing to 700 K for about 600 s. The preparation was checked with Auger electron spectroscopy, ultraviolet photoemission spectroscopy, low-energy electron diffraction, and two-photon photoemission spectroscopy (2PPE). The metals were evaporated at room temperature at a rate of $\approx0.5$ ML per minute (1 ML $=1.53\times10^{15}$ atoms/cm$^2$) by electron bombardment of Fe or Co rods with 2-mm diameter. The pressure during evaporation did not exceed $4\times10^{-8}$ Pa. The coverages were controlled by a built-in flux monitor in connection with a calibrated quartz microbalance. After evaporation, the crystal was cooled down to 100 K within 15 min in order to reduce

 

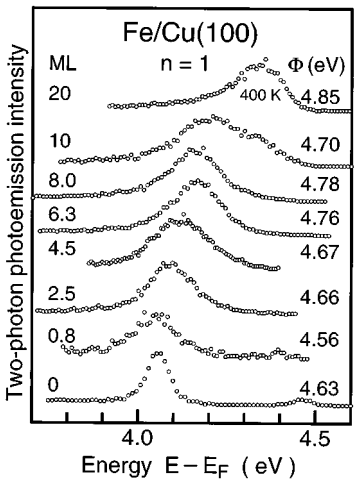


FIG. 1. Series of 2PPE spectra of Cu(100) with increasing iron coverage. The spectra are normalized to maximum count rate and are plotted relative to the Fermi energy $E_F$. On the left side the coverage and on the right side the work function $\Phi$ are shown, respectively.

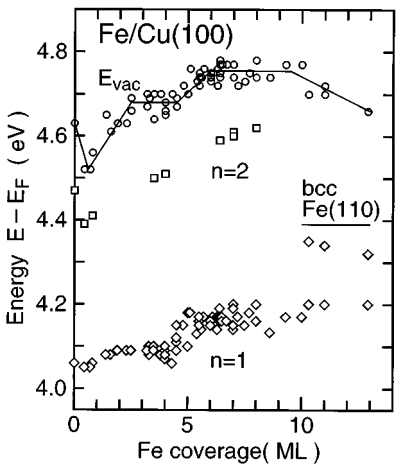


FIG. 2. Energies of the image states as a function of the iron coverage on Cu(100) (diamonds: $n=1$, squares: $n=2$). The vacuum level is represented by circles, the solid line is a guide to the eye. The horizontal line marked bcc Fe(110) stands for the energetic postion of the $n=1$ image state on Fe(110).

surface diffusion[25,26] and to enable 2PPE measurements with a reduced low-energy cutoff.[24] The work function was determined from the energetic width of the photoelectron spectra.

### III. IMAGE STATES ON Fe/Cu(100)

Two-photon photoemission spectra for the clean Cu(100) surface and the iron-covered surface are shown in Fig. 1. The spectra are plotted relative to the Fermi energy $E_F$ and each spectrum is normalized to maximum height. On the left side the respective coverage is given in monolayers and on the right side the work function $\Phi$ is shown. On Cu(100) the lowest image states numbered by $n=1$ and $n=2$ are detected at $4.06\pm0.03$ eV and $4.46\pm0.03$ eV above $E_F$, respectively. This is in agreement with previous studies.[11,27]

At an iron coverage of 0.8 ML we still detect two image states. Compared to the spectrum for the clean surface, the intensity is much lower as can be inferred from the larger noise of the data. The energy of the $n=1$ state is unchanged, but the peak width is considerably larger. The $n=2$ state has shifted to lower energies by the same amount as the decrease of the work function.

At 2.5-ML coverage we observe electrons out of an image state at a slightly higher energy than the one from clean Cu(100). The linewidth is also increased. At 4.5 ML the peak is even broader and asymmetric with a tail at the high-energy side. The spectrum at this coverage can be explained as a weighted sum of the image state spectra from the 2.5 and 6.3-ML films. This indicates a continuous change in the surface morphology. Between 5 and 10 ML iron we detect the image states with the highest count rate and smallest linewidth for all iron films. This is a sign for the best-ordered films in the investigated coverage regime. The line shape and in particular its dependence on the polarization of the exciting light will be discussed in more detail in Sec. IV.

At a coverage of 10 ML we can observe another transition in the appearance of the spectra: In addition to the image state of fcc iron we see another feature in our spectra at around 4.35 eV relative to the Fermi level. From its energetic position, this state can be interpreted as an $n=1$ image state from bcc Fe(110) (Ref. 22). At even higher coverages the surfaces have to be annealed to 400 K for 60 s in order to obtain satisfactory count rates. One can no longer detect the fcc state at these coverages.

The results for all films measured at various photon energies are compiled in Fig. 2. The energetic position of the detected states relative to $E_F$ are plotted versus the iron coverage. The diamonds symbolize the $n=1$ and the squares the $n=2$ image states. The $n=2$ data for Fe coverages above 2 ML were obtained using higher photon energies than for the spectra shown in Fig. 1. The circles indicate the measured values for the vacuum energy $E_{\mathrm{vac}}$. The solid line is a guide to the eye through the scattered data points.

One can distinguish four different coverage regimes: (1) 0–1 ML: $n=1$ image state at 4.06 eV, work function drops $\approx0.1$ eV below the Cu(100) value. (2) 2–4 ML: $n=1$ image state at 4.09 eV, work function $\approx4.68$ eV. (3) 5–10 ML: $n=1$ image state at 4.17 eV, work function $\approx4.76$ eV. (4) $\geqslant10$ ML: $n=1$ image states at 4.20 eV and $\approx4.35$ eV, work-function decrease.

The adsorption of iron on a Cu(100) surface at room temperature leads for small coverages to an extremely inhomogeneous surface.[25] This results in a significant lowering of the work function compared to the clean copper surface, which affects mainly the $n=2$ state. Because these states are further away from the surface, they average over larger areas than the $n=1$ states, which feel a local work function.[13] From 2–3 ML on, the iron atoms form a film with well-defined image states and work function but the first layer is still corrugated.[28] This corrugation leads to a reduced work function of the iron layers of 0.08 eV compared to the films between 5 and 10 ML, which show no corrugation of the first layer.[29] At a coverage slightly above 4 ML we observe the transition between these two fcc film morphologies through the variation of the energetic position of image states as well as the variation of the work function. Due to their small linewidth and high count rate, we attribute the image states between 5 and 10 ML to the best-ordered films in this study.

TABLE I. Experimental values for the work function Φ and the energies of the $n=1$ image states. All energies are given in eV relative to $E_F$. The experimental error is about ±0.03 eV. The theoretical values for the energies of the $n=1$ image states result from calculations within a one-dimensional scattering model (Ref. 32).

| | | | Clean | 2 ML | 4 ML | 6 ML | 8 ML | Film |
|---|---|---|---|---|---|---|---|---|
| Fe | Expt. | Φ | 4.63 | 4.68 | 4.68 | 4.76 | 4.76 | |
| on | Expt. | $n=1$ | 4.06 | 4.09 | 4.09 | 4.17 | 4.17 | 4.35 |
| Cu(100) | Theor. | $n=1$ | 4.11 | 4.21 | 4.22 | 4.30 | 4.30 | |
| | | | Clean | 1 ML | 2 ML | 3 ML | 4 ML | Film |
| Co | Expt. | Φ | 4.63 | 4.66 | 4.72 | 4.72 | 4.78 | 4.78 |
| on | Expt. | $n=1$ | 4.06 | 4.16 | 4.17 | 4.18 | 4.19 | 4.19 |
| Cu(100) | Theor. | $n=1$ | 4.11 | 4.16 | 4.23 | 4.23 | 4.29 | 4.30 |

Therefore, these films were used to study the exchange splitting of the image states in Sec. IV. At a coverage of around 10 ML we observe another transition. This is the changeover from the fcc into the bcc film morphology of (110) orientation which has been observed before.[30,31] It is interesting to note that the image-state energy of 4.35 eV is close to the value measured on the (110) surface of a fcc Fe bulk sample.[22] The significantly lower work function indicates a considerable roughness of the films. As a first conclusion, we see that we are able to follow the coverage-dependent morphologies of Fe/Cu(100) films reported by structural investigations.[25]

The work function and energy position of the $n=1$ image state for monolayer coverages are listed in Table I. The results for the energies of the $n=1$ image states are compared to calculations with a one-dimensional scattering model[21,32] using spin-averaged band edges from a band-structure calculation.[33] The calculated energies are slightly higher than the experimental values with increasing deviations for higher coverages. The same situation has been found for other ferromagnetic surfaces.[22] Possible explanations are self-energy effects[21] or a different position of the effective image plane at surfaces with *d*-electron screening.

In the case of Co/Cu(100), our measurements are compatible with the layer-by-layer growth (at least from the second layer on) of cobalt on Cu(100) reported in the literature.[34–41] In particular, there were no signs of a transition from the fcc morphology to the hcp structure, which is at room temperature favored by cobalt. This was checked for coverages up to 11 ML. The energy of the image states as well as the work function for several coverages are also given in Table I. For thick films the work function and the energy of the image states are significantly lower than the corresponding values measured on the (0001) surface of a hcp Co bulk sample.[22]

## IV. EXCHANGE SPLITTING OF IMAGE STATES

The results of the preceding section gave no clear indication for a splitting of the image states into a pair of states with majority and minority spin orientation. The larger linewidth of the spectra in certain coverage regimes could be explained by a poorer surface quality or mixtures of different

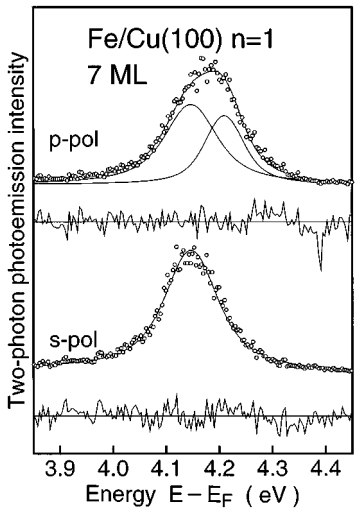


FIG. 3. Spectra of the $n=1$ image state for 7 ML Fe/Cu(100) plotted relative to the Fermi energy $E_F$ and normalized to maximum count rate. For the upper spectrum, the excitation into the image state was done by *p*-polarized light, whereas *s*-polarized light was used for the lower spectrum. The solid lines show the fit functions and the residuals below each spectrum.

surface structures. To our knowledge, no experimental or theoretical investigations on the spin splitting of the image states on fcc Fe(100) have been performed. It seems, therefore, reasonable to expect for Fe/Cu(100) an exchange splitting of the image states around 57 meV as has been measured for bcc Fe(110) (Ref. 17). The most promising coverage for a search for the exchange splitting of the image states is in the range between 5 and 10 ML, where the narrowest peaks are observed (see Fig. 1). Similar to the case of the close-packed ferromagnetic surfaces[22] the intrinsic linewidth of the spectra is larger than the exchange splitting, so only an upper limit could be obtained from a line-shape analysis of the experimental data.

Additional information can be obtained by a variation of the polarization of the incident light. Figure 3 shows two 2PPE spectra of the $n=1$ image state on 7-ML Fe/Cu(100). Each spectrum is normalized to a maximum count rate and plotted versus the energy relative to the Fermi level. For the lower spectrum, we used *s*-polarized light for the excitation of an electron from the bulk bands into the image state and for the upper spectrum we used *p*-polarized light for that step. The wavelength of the ionizing light was 560 nm for both spectra. The lower spectrum shows an image state at lower energy relative to $E_F$ and with smaller linewidth than the upper one. The excitation by *p*-polarized light is much more efficient and leads to a significantly larger electron emission. Because the shift and broadening in the upper spectrum were observed also for lower laser intensities and at other photon energies, we can rule out that they are caused by space-charge effects. Such effects could be definitely excluded only for films in the coverage range between 5 and 10 ML. At other coverages the poorer film quality leads to a lower image-state intensity, an increased linewidth, and a larger background of low-energy electrons. This makes the identification of small shifts and broadening in the spectra difficult.

The experimental results can be analyzed as a single peak

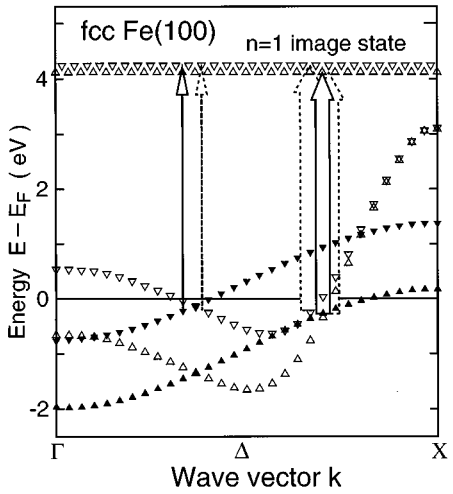


FIG. 4. Band structure of fcc Fe(100) along $\Delta$ (after Ref. 42). Excitation into the image states can occur only from energy bands of $\Delta_1$ (open symbols and dashed arrows) and $\Delta_5$ (filled symbols and solid arrows) symmetry. Upward and downward triangles represent majority and minority spin states, respectively. The exchange splitting of the image states is exaggerated. From the widths of the arrows the different occupation of the image states for excitation with *s*-polarized (solid arrows) and *p*-polarized (solid and dashed arrows) light can be inferred.

excited by *s*-polarized light and by the observation of an additional peak for *p*-polarized light. Following this interpretation, we have performed line fits in which the weighted $\chi^2$ sum gets minimized. We fitted the lower spectrum with a Lorentzian function for the intrinsic lifetime broadening of the image state convoluted with a Gaussian function for the analyzer resolution.[24] The resulting energetic position and linewidth were then fixed as input for the fit function for the upper spectrum. This leads to the significant fitting of an additional state at higher energies and to an improvement over fits with only one peak. The solid lines represent the resulting fit functions. For each fit we also show the residuals, i.e., the deviation of the fit function from the data points weighted by the error of the individual data points. Following this procedure we obtain an exchange splitting of the first image state on 7-ML fcc Fe/Cu(100) of $65\pm15$ meV averaged over several preparations. The coverage dependence of this splitting could not be investigated because only films in this coverage regime yield spectra with sufficiently narrow linewidth and low background. For other coverages it is also difficult to avoid space-charge broadening in the spectra with *p* polarization for laser intensities where sufficient signal could be obtained with *s*-polarized light. For 6 ML of Co on Cu(100) a value of $55\pm10$ meV for the exchange splitting of the $n=1$ image state is obtained.

The most straightforward interpretation of the two peaks observed in the spectra of Fig. 3 is that we see only the majority image state in the lower spectrum and both majority plus minority image states in the upper spectrum. Now the interesting question is why should one observe only the majority image state when using *s*-polarized light for the excitation of electrons into the image states and the majority and minority states when using *p*-polarized light? To answer this question, we plot in Fig. 4 the band structure of Fe/Cu(100) along the $\Gamma\Delta X$ (100) direction (after Ref. 42). Shown are only bands of $\Delta_1$ and $\Delta_5$ symmetry by open and filled symbols, respectively. Due to dipole selection rules[43] these states are the only possible initial states for excitation of image states (of $\Delta_1$ symmetry) in our experimental setup. Upward triangles stand for majority states, downward triangles for minority states. Image states are surface states and show no dispersion along the direction of the surface normal. Their exchange splitting is exaggerated for the sake of better visibility. Due to the conservation of the electron spin in optical excitations, the majority image state can only be occupied by electrons from majority states and the minority image state only by electrons from minority states.

With *s*-polarized light as indicated by the solid arrows in Fig. 4 the image states can be populated only from $\Delta_5$ states due to dipole selection rules.[43] The excitation of the states with the different spin orientations from the $\Delta_5$ bands occurs at different wave vectors, which implies a different periodicity of the wave function. The wave function of the image state in the metal is an exponentially decaying standing wave with the same periodicity as the bulk states at the zone boundary *X*. The matrix element for the optical transition from bulk bands into the image state has its maximum for the wave vector at *X* and decreases towards $\Gamma$. This argument takes into account only the periodicity of the wave function and should be a good approximation for the slowly dispersing *d* bands where the orbital character of the wave function does not depend strongly on the wave vector. These considerations explain why the emission from the majority-spin image state dominates the spectrum for *s*-polarized light as indicated by the solid arrows in Fig. 4 in agreement with the experiment.

For *p*-polarized light the polarization vector has components parallel and perpendicular to the surface normal, because the laser beam hits the surface under an angle of 45° in our experimental setup. The image states can, therefore, be populated from initial states with $\Delta_1$ (dashed arrows) or $\Delta_5$ symmetry with *p*-polarized light.[43] However, as indicated qualitatively by the width of the arrows in Fig. 4, the excitation of the image states from the slowly dispersing *d* states is much less efficient than from the strongly dispersing *sp* bands of $\Delta_1$ symmetry. This can be seen directly in the experiment, because the intensity using *s*-polarized light is smaller than for *p*-polarized light, where excitation from the $\Delta_1$ bands contributes. The wave functions of the image states are exponentially decaying solutions in the *sp* band gap of the bulk band structure. The overlap with the wave functions of the *sp* bulk bands of similar character is large. This leads to a strong excitation of the image states from the *sp* bulk bands compared to the excitation from *d* bands. At the photon energy used, the image states are excited from bands close to the Fermi level $E_F$. As can be seen in Fig. 4, the exchange splitting of the *sp* bands of $\Delta_1$ symmetry in the relevant *k* range is quite small. Because the wave vector and wave function are almost identical for the two spin orientations, the matrix element for the transition into the image states should be in first approximation independent of the spin direction. These considerations and the negligible contribution by the excitation from *d* bands explain why we observe both majority and minority image states with *p*-polarized light.

These arguments justify our assumption that the spectra

obtained with $s$-polarized light show only the majority image state, whereas spectra using $p$-polarized light show the majority and the minority state. It should be emphasized that the exchange splitting of the electronic states exists for ferromagnetic samples independent of the magnetization. The polarization effect has been observed without magnetizing the sample by an external field and identical results are observed for magnetized and unmagnetized films. The values obtained for the exchange splitting of $65\pm15$ meV and $55\pm10$ meV for Fe and Co films on Cu(100) are close to the values reported for close-packed surfaces of bulk crystals,[17,22] which agree with theoretical estimates.[11,19,20] Experimental or theoretical data for the exchange splitting of the image states on fcc films are not available. Our results are in agreement with the general trend that the exchange splitting for Co is smaller than for Fe (Refs. 11 and 22). For a calculation with a one-dimensional scattering model[32] we scaled theoretical values for the exchange splitting of the edges of the $sp$ band gap[33] to match the published $d$ band splitting of fcc Fe(100) (Ref. 42). We obtain an exchange splitting of the first image state of 11 and 19 meV on fcc Co and Fe, respectively. These numbers lie well below the experimental values, much like in the case of the bulk surfaces.[11]

From our data analysis we also obtain the intrinsic linewidth for the various $n=1$ image states. The majority $n=1$ state of 7-ML Fe/Cu(100) has a linewidth of $98\pm12$ meV and the minority state a linewidth of $71\pm20$ meV. This compares to the values for 6-ML Co/Cu(100) of $82\pm9$ meV and $90\pm17$ meV for the majority and minority state, respectively. So within the error limits no spin dependence of the intrinsic linewidth of the $n=1$ image states on Fe/Cu(100) and on Co/Cu(100) is observed. Such a dependence has recently been found for the bcc Fe(110) surface.[17] These authors report linewidths of $70\pm10$ meV for the majority $n=1$ image state and $140\pm10$ meV for the minority state. We would like to note here that the two-photon photoemission data of Ref. 22 and recent measurements[44] for bcc Fe(110) are not compatible with such a large linewidth of the minority states and favor approximately equal linewidths for the image states of both spin orientations.

## V. SUMMARY AND OUTLOOK

In this paper we have shown how the coverage-dependent morphology of Fe/Cu(100) can be monitored by the two-photon photoemission from image states. This is possible because these states are localized only some angstroms in front of the surface and are therefore strongly influenced by the local potential in front of the surface. With different linear polarizations of the exciting light we observe different peak positions and linewidths of the image states. The interpretation as an effect of a spin-selective excitation leads to a determination of the exchange splitting of the image states. This proves that these surfaces are ferromagnetic in contrast to Hezaveh *et al.*[6] and Macedo and Keune,[7] but in agreement with Thomassen *et al.*[5] and Detzel *et al.*[8] The values for the exchange splittings are in agreement with other reports. The intrinsic linewidths of the image states are in the range of previous reports for close-packed surfaces of ferromagnetic materials.[17,22]

Of particular importance is the fact that it is not necessary to magnetize the sample for these measurements in contrast to other spin-dependent spectroscopies. The spin-selective excitation process works for each domain of magnetization on the sample separately. This opens the possibility to search for a possible exchange splitting in systems lacking magnetization, such as ferromagnetic surfaces above the Curie temperature or small islands.

## ACKNOWLEDGMENTS

We acknowledge stimulating discussions with Professor W. Steinmann. This work was supported in part by the Deutsche Forschungsgemeinschaft (DFG) through SFB 338.

*Author to whom correspondence should be sent. Present address: Lehrstuhl für Festkörperphysik, Universität Erlangen-Nürnberg, Staudtstrasse 7, D-91058 Erlangen, Germany. Electronic address: fauster@fkp.physik.uni-erlangen.de

[1] O. Haase, Z. Naturforsch. A **14**, 920 (1959).
[2] W. A. Jesser and J. W. Matthews, Philos. Mag. **15**, 1097 (1967).
[3] M. Onellion *et al.*, Surf. Sci. **179**, 219 (1987); S. H. Lu *et al.*, *ibid.* **209**, 364 (1989).
[4] H. Glatzel, Th. Fauster, B. M. U. Scherzer, and V. Dose, Surf. Sci. **254**, 58 (1991).
[5] J. Thomassen *et al.*, Phys. Rev. Lett. **69**, 3831 (1992).
[6] A. A. Hezaveh, G. Jennings, D. Pescia, and R. F. Willis, Solid State Commun. **57**, 329 (1986).
[7] W. A. A. Macedo and W. Keune, Phys. Rev. Lett. **61**, 475 (1988).
[8] T. Detzel, M. Vonbank, M. Donath, and V. Dose, J. Magn. Magn. Mater. **147**, L1 (1995).
[9] M. Donath, Surf. Sci. Rep. **20**, 251 (1994).
[10] V. Dose, Surf. Sci. Rep. **5**, 360 (1985).
[11] W. Steinmann and Th. Fauster, in *Laser Spectroscopy and Photochemistry on Metal Surfaces*, edited by H. L. Dai and W. Ho (World Scientific, Singapore, 1995), Chap. 5, p. 184.
[12] N. Fischer *et al.*, Phys. Rev. B **47**, 4705 (1993).
[13] R. Fischer *et al.*, Phys. Rev. Lett. **70**, 654 (1993).
[14] W. Wallauer and Th. Fauster, Surf. Sci. **331-333**, 731 (1995).
[15] K. Starke, K. Ertl, and V. Dose, Phys. Rev. B **45**, 6154 (1992).
[16] F. Passek and M. Donath, Phys. Rev. Lett. **69**, 1101 (1992).
[17] F. Passek, M. Donath, K. Ertl, and V. Dose, Phys. Rev. Lett. **75**, 2746 (1995).
[18] F. J. Himpsel, Phys. Rev. B **43**, 13 394 (1991).
[19] M. Nekovee, S. Crampin, and J. E. Inglesfield, Phys. Rev. Lett. **70**, 3099 (1993).
[20] G. Borstel and G. Thörner, Surf. Sci. Rep. **8**, 1 (1988).
[21] Th. Fauster and W. Steinmann, in *Photonic Probes of Surfaces*, Electromagnetic Waves: Recent Developments in Research, Vol. 2, edited by P. Halevi (North-Holland, Amsterdam, 1995), Chap. 8, p. 347.
[22] R. Fischer *et al.*, Phys. Rev. B **46**, 9691 (1992).
[23] H. Glatzel, R. Schneider, Th. Fauster, and V. Dose, Z. Phys. B **88**, 53 (1992).
[24] S. Schuppler, N. Fischer, Th. Fauster, and W. Steinmann, Appl. Phys. A **51**, 322 (1990).
[25] Th. Detzel, N. Memmel, and Th. Fauster, Surf. Sci. **293**, 227 (1993).
[26] A. Rabe, N. Memmel, A. Steltenpohl, and Th. Fauster, Phys. Rev. Lett. **73**, 2728 (1994).

[27] K. Giesen *et al.*, Phys. Rev. B **35**, 971 (1987).
[28] S. Müller *et al.*, Phys. Rev. Lett. **74**, 765 (1995).
[29] P. Bayer, S. Müller, P. Schmailzl, and K. Heinz, Phys. Rev. B **48**, 17 611 (1993).
[30] P. Schmailzl *et al.*, Surf. Sci. **312**, 73 (1994).
[31] J. Giergiel *et al.*, Surf. Sci. **310**, 1 (1994).
[32] Th. Fauster, Appl. Phys. A **59**, 639 (1994).
[33] J. Noffke (private communication).
[34] L. Gonzalez *et al.*, Phys. Rev. B **24**, 3245 (1981).
[35] A. Clarke *et al.*, Surf. Sci. **187**, 327 (1987).
[36] D. Kerkmann, Appl. Phys. A **49**, 523 (1989).
[37] J. J. de Miguel *et al.*, Surf. Sci. **211/212**, 732 (1989).
[38] C. M. Schneider *et al.*, Phys. Rev. Lett. **64**, 1059 (1990).
[39] H. Li and B. P. Tonner, Surf. Sci. **237**, 141 (1990).
[40] A. K. Schmid and J. Kirschner, Ultramicroscopy **42-44**, 483 (1992).
[41] M. T. Kief and W. F. Egelhoff, Jr., Phys. Rev. B **47**, 10 785 (1993).
[42] G. J. Mankey, R. F. Willis, and F. J. Himpsel, Phys. Rev. B **48**, 10 284 (1993).
[43] W. Eberhardt and F. J. Himpsel, Phys. Rev. B **21**, 5572 (1980); **23**, 5650 (1981).
[44] Chr. Reuß, U. Thomann, W. Wallauer, and Th. Fauster (unpublished).